Quantifying the Influence of Motion Damping on Co-Located Wind and Wave Energy Devices

E. Ritchie, and E. Gubesch

Abstract—**Offshore renewable energy holds the potential to satisfy growing demands for global, clean energy production. The co-existence of offshore wind and wave energy conversion technologies presents a compelling opportunity for sustainable energy generation at sea. This paper investigates the integration of a co-located point absorbing wave energy converter (WEC) with a monopile supported offshore wind turbine (OWT). Numerical simulations were validated with experimental data and were then used to investigate the hydrodynamic interactions of the two renewable energy systems, addressing the influence of WEC motions and damping on OWT wave loading. The full-scale geometry of the WEC and OWT were sized according to conditions at the proposed *Star of the South* wind farm in Gippsland, Victoria, Australia. The study found that the WEC's heave and surge degrees of freedom are highly influential, with a 33% reduction in surge force on the OWT foundation in operational irregular sea states. Furthermore, highly energetic irregular sea states with a 100-year return period saw surge forces reduced by 19%. Although a fixed WEC operating purely as a wave mitigation device was beneficial, utilising a heave and surge coupled WEC proved to be a far more effective method for load reduction.**

Keywords— **Co-located wave energy and offshore wind structures, offshore renewable energy, reducing wave loading on offshore structures.**

I. Introduction

Offshore renewable energy (ORE) devices hold the potential to satisfy a considerable portion of the global demand for clean, sustainable energy. Offshore wind is currently the most developed and commercialised technology in the ORE industry, with wave energy converters (WECs) beginning to surface as an additional method for harnessing ocean wave energy. However, the wave energy sector is far from its full commercial potential. Although rich in energy resources, the harshness of the ocean environment poses a significant challenge to successful implementation of many ORE technologies. Critically, ORE devices must be capable of surviving constant cyclical loads caused by wind, wave and current forces. Due to this, the additional design and fabrication costs associated with survivability of ORE devices are high. Balancing capital and operational expense with profitable energy yield is the main obstacle that any ORE device must overcome in order to become commercially viable [1]. Therefore, reducing environmental loads on ORE devices is particularly important.

Offshore wind turbines experience significant environmental loading generated by wind forces acting on the turbine rotor and tower. Secondary loading is generated by ocean waves impacting the OWT foundation. These highly cyclic wave loads increase material and structural fatigue, resulting in increased capital expenses to combat these effects. As strong wind resources are desirable for energy production, the only means of reducing environmental loads without decreasing production is through mitigation of ocean wave forces. A potential avenue for this may be through co-location of wind and wave ORE devices. Co-located systems combine offshore wind and wave energy devices through independently founded systems that may share marine area, grid connection and supporting infrastructure. This differs from hybrid energy systems which are single-founded marine structures (fixed or floating) comprising more than one ORE device [2]. Engineering economically sustainable WEC devices capable of withstanding ocean conditions is particularly challenging and has significantly slowed development progress. WEC devices are designed with natural frequencies corresponding to the operational wave period at the intended installation site. Although this maximises WEC energy production, it places the WEC in a highly energetic state of cyclic motion for its entire lifespan, thus increasing system wear. Although various WEC devices have progressed from concept to prototype, the wave energy sector as a whole is yet to become a large-scale

Part of a special issue for ICOE 2024. Manuscript submitted 18 July 2025; Accepted 18 July 2025. Published 13 April 2026.

E. Ritchie is with BridgePro Engineering Pty. Ltd, Latrobe, Tasmania, Australia (e-mail: ethanr0@utas.edu.au).

E. Gubesch is with the Australian Maritime College, University of Tasmania, Newnham, Tasmania, Australia (e-mail: eric.gubesch@utas.edu.au).

Digital Object Identifier: https://doi.org/10.36688/imej.8.499-508

commercially viable option for energy production [3]. The effect of co-located OWT and WEC devices may provide mutual benefit in the reduction of loads on OWT structures with simultaneous increases in energy production from the combined OWT and WEC system. Importantly, the ability for combined OWT and WEC systems to share common ORE infrastructure such as offshore substations and subsea cabling may provide an avenue for wave energy devices to become an economically viable energy solution.

Initial investigations into hybrid floating WEC and OWT systems for the purpose of motion suppression were conducted by Borg et al. [4]. This paper introduced the concept of using a WEC to reduce floating motions rather than implementing damping devices to dissipate ocean waves. Initial findings suggested additional energy increase for the system could be made through the WEC while improving the cost effectiveness of the system. Studies by Gaughan et al. [5] and Zhao et al. [6] confirmed WEC devices are able to reduce floating OWT motions significantly, concluding that co-located ORE technologies can provide a more predictable, less variable ORE source. Zhao et al. [6] went on to suggest that a hybrid OWT WEC system could reduce wind turbine pitch motion by approximately 50-60% for the average maximum wave conditions with increased power production of 14%. Similar results were also shown by Hu et al. [7], demonstrating the integrated WEC not only increased the total power of the OWT/WEC hybrid but also reduced the pitch motion of the OWT. These studies neglected hydraulic and electrical losses at the generator between OWT and WEC. Meng et al. [8] investigated simultaneous power generation and reduction of motions using a small array of WEC devices that were controlled to generate wave field interference such that the motion of a floating OWT is suppressed. Recommendations for further studies of variable wind and wave directions with layout reconfigurations were made to reduce wave amplitude in the OWT array.

Astariz [9] investigated the layout of WEC devices and shielding effects for an OWT farm using fixed overtopping WEC devices. The aim of the study was to quantify the wave height reduction achieved within a co-located wave-wind farm. Multiple layouts of large scale WEC farms (acting as breakwaters) were investigated with small amplitude 1.5 m regular waves. Arrays of WECs with small spacing between converters demonstrated the best results in terms of wave height reduction. Astariz [10] continued to find that peripherally distributed arrays achieve good results in wave height reduction, however, uniformly distributed WEC arrays were superior in reduction of wave height over the entire OWT farm.

An experiment conducted in 2022 by the Australia-China Joint Research Centre for Offshore Wind and Wave Energy Harnessing involved a theoretical study into the hydrodynamic interactions between a heave-only co-located WEC and a bottom-fixed OWT foundation [11,12]. This study examined the effect of the WEC's heave motion at various phases on the surge forces and overturning moments of a fixed offshore wind turbine foundation. Results from this study indicate that fixed OWT surge forces can be reduced by up to 40%; however, the WEC may require a reactive control system to ensure its heave motions maintain optimal phase. The study considered the WEC to be a heave-only body; however, when moored-floating offshore, the WEC will likely display strong heave and surge coupling depending on the mooring and power take-off (PTO) arrangement. Additionally, the sizing of the WEC and OWT in [11,12] may not be directly comparable to realistic deployment at full-scale.

While previous studies [11,12] demonstrate positive hydrodynamic interactions between co-located OWTs and heave-only WECs, further investigation is needed to understand how coupled heave and surge motions of the WEC influence the forces and moments experienced by a OWT foundation under realistic deployment.

This paper presents the results of a numerical study into the effects of motion damping for a full-scale co-located point absorber WEC and OWT foundation. The full-scale geometry of the WEC and OWT were sized according to conditions at the proposed *Star of the South* wind farm in Gippsland, Victoria, Australia. The change in resultant loading on the OWT due to the co-located WEC has been investigated with particular focus on heave and surge motions at various damping levels. The remainder of the paper is structured as follows: Section 2 outlines the development and validation of the numerical model (Ansys AQWA) used in this study. Section 3 presents detailed analysis, and a description of the results generated through the numerical simulations. Finally, conclusions and recommendations for further work are presented in Section 4.

II. Methodology

Research in this paper builds on work conducted by the Australia-China Joint Research Centre for Offshore Wind and Wave Energy Harnessing [11,12], which experimentally investigated hydrodynamic interactions between a co-located WEC and OWT. Conducted at the Australian Maritime College Model Test Basin, the scale model construction consisted of a 760 mm diameter carbon steel pipe and a 500 mm diameter fibreglass buoy reinforced with an internal plywood structure. The larger structure was fixed to the test basin floor, representing the monopile OWT foundation, with the secondary structure representing the point absorbing WEC. Fig. 1 illustrates the experimental setup and geometry of the tested models.

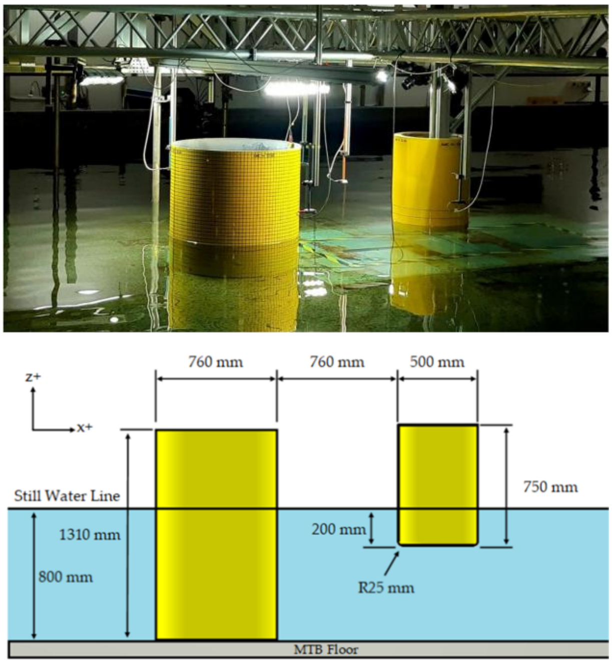

Fig. 1. Top: Experimental setup measuring diffraction forces on the WEC and OWT in [11]. Bottom: General arrangement and principal dimensions of the experimental models. Waves approach from the right-hand side.

A. *Numerical validations*

Rigorous numerical validations were conducted to confirm the hydrodynamic modelling capabilities of the Ansys AQWA potential flow solver. Four independent experimental datasets were used during validation to determine appropriate numerical settings for the body of research presented in this article. The numerical validations were split into the following categories:

1. A fixed bottom-mounted OWT foundation: This validation evaluated surge forces and pitch moments on the OWT.
2. Co-located OWT with a fixed WEC: This validation was designed to evaluate multi-body interactions and resultant surge motions and pitch forces on the OWT.
3. Heaving WEC motions: This validation evaluated the motions and damping characteristics of a heave-constrained cylinder.
4. A taut-moored floating sphere: This validation evaluated heave and surge coupled motions of a floating WEC and resembles a single-point mooring configuration.

Each condition was specifically selected to verify AQWA's modelling capability to replicate heave and surge motions of a WEC and to produce accurate OWT pitch moments and surge forces for each scenario. Where appropriate, the effect of both regular and irregular wave conditions was investigated during validation, as both conditions are necessary for a well-developed numerical model.

Validation 1: Fixed OWT

This validation evaluated numerical settings to accurately model the surge forces and pitch moments on a fixed OWT foundation. A description of the experimental setup and data used for this validation can be found in [11].

Regular waves were generated via the AQWA hydrodynamic response module to coincide with the experimental conditions. The results for Validation 1 (Fig. 2) demonstrate the accuracy between the experimental data and numerical simulations. The numerical simulations over-predict surge forces by an average of 3.8% and under-predict pitch moment on the wind turbine foundation by 7.7%. This level of difference is acknowledged as a limitation of the numerical model, as potential flow solvers neglect flow irregularities such as turbulence, vorticity and boundary layer effects which may affect loading on the OWT. Nevertheless, the difference is acceptable for this validation.

Hydrodynamic responses to irregular wave fields were investigated by importing the incident experimental surface elevation data into the AQWA solver directly as a user-defined wave. This method was selected so the numerical responses could be directly compared to the experimental data (Fig. 3). This resulted in a coefficient of determination (R^2) of 0.999 between the power spectral density of the experimental and numerical surface elevations; however, it clearly over-predicted the magnitude of the time domain and spectral response of the OWT surge force ($R^2 = 0.961$) and pitch moments ($R^2 = 0.954$).

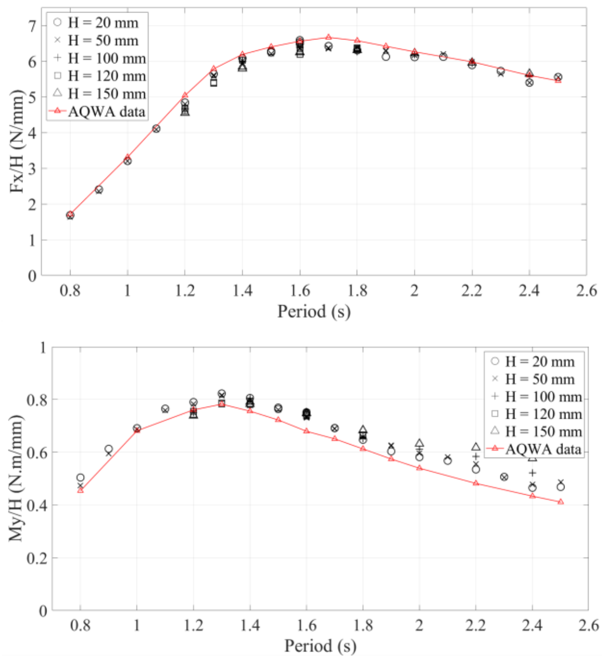

Fig. 2. Validation results for a fixed OWT. Top: OWT surge force, Bottom: OWT pitch moment.

Validation 2: Fixed OWT and WEC

This validation evaluated numerical settings to accurately model the surge forces and pitch moments on a fixed OWT foundation when a fixed WEC is positioned

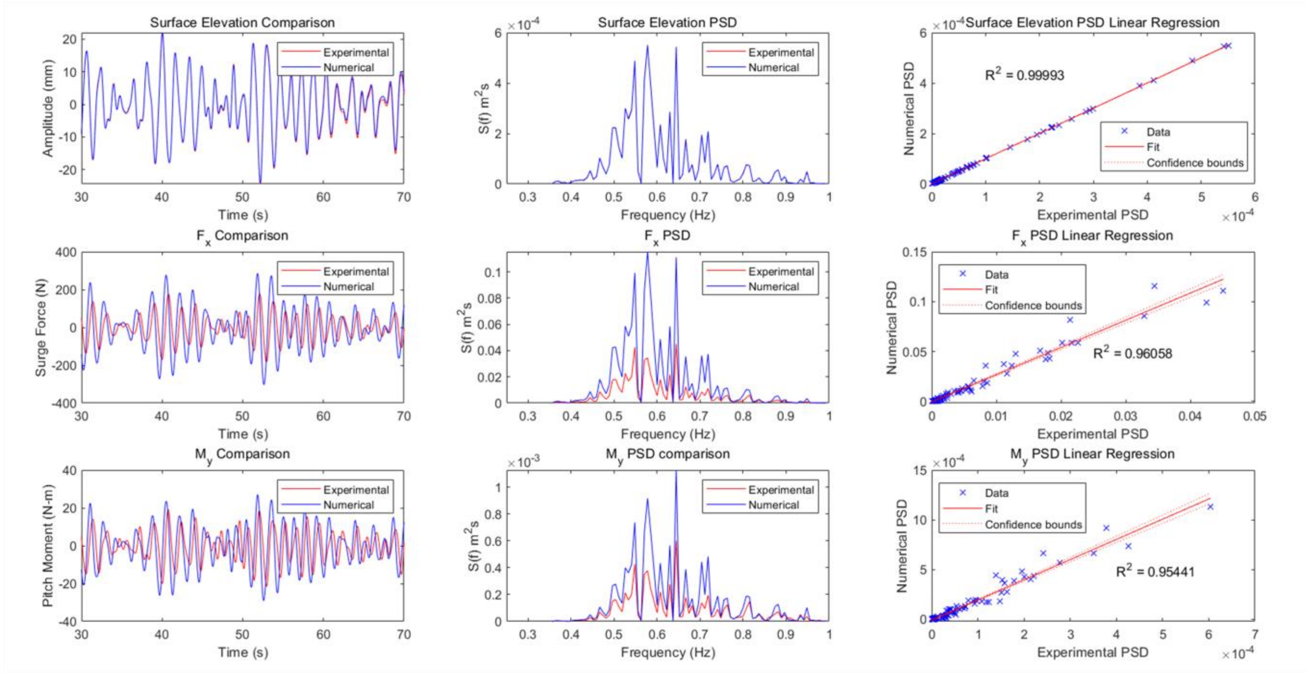

Fig. 3. Irregular wave validation comparing experimental and numerical responses. Here the target surface elevation is accurately replicated, however the OWT surge forces and pitch moments are under predicted.

between the OWT foundation and incoming waves. A description of the experimental setup and data used for this validation can be found in [11]. See Fig. 1 for reference.

The results for Validation 2 can be found in Fig. 4. Consistent with Validation 1, the AQWA model slightly over-predicted surge forces on the OWT by an average of 5.0%. However, the pitch moment results show good agreement, with an average prediction difference of 1.1%.

Validation 3: Heaving WEC

For Validation 3, experimental data from a 2019 study [13] was used to verify wave-induced vertical motions of the WEC. This study investigated the hydrodynamic performance of a heave-only cylindrical buoy (1-DOF, z-direction) in free-floating and sprung conditions, which mimic the buoy's motion as influenced by a PTO system. The numerical model was set up to replicate the experimental conditions for both sprung and free-floating scenarios. The results of the AQWA simulations demonstrate good agreement between the numerical decay model and the experimental data (Fig. 5). Additional damping required to accurately model the heaving WEC motions was calculated using the method outlined in [14] regarding additional viscous damping for a floating oscillating water column WEC. The additional viscous damping mitigates excess WEC motions due to the zero-viscosity assumption within potential flow theory. Once the decay test had been successfully completed, the numerical model was further validated against both regular and irregular incident waves, verifying AQWA's ability to model a heaving WEC, with the heave response motions considered to be a highly accurate representation of the experimental data.

Validation 4: WEC heave and surge coupled motion

For Validation 4, experimental data [15, 16] from a 2022 study was used to investigate the sensitivity of numerical damping parameters of a taut-moored floating sphere during free body decay tests. The AQWA model was found to be sensitive to mooring line stiffness, activated degrees of freedom (DOF), and the initial starting position. However, after refinement of the mooring arrangement, good agreement between the numerical model and the experimental data was achieved, where a difference of 1.1% in surge and 5.9% in heave was observed.

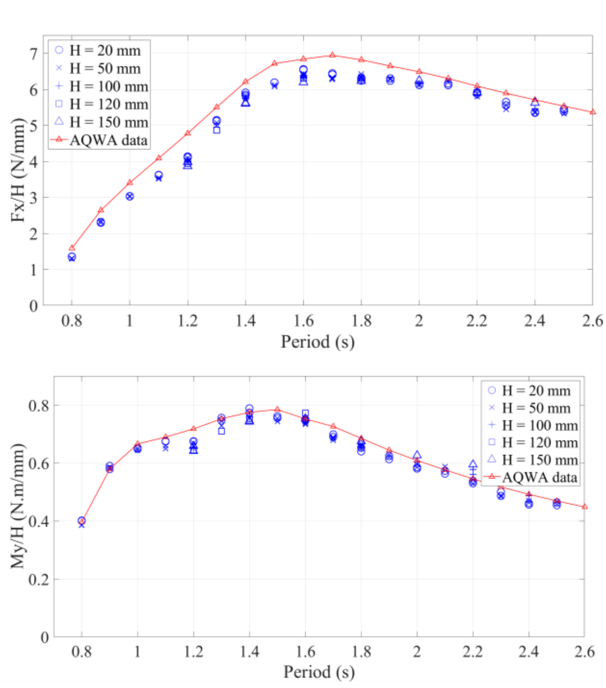

Fig. 4. Validation results for a co-located OWT and fixed WEC. Top: OWT surge force, Bottom: OWT pitch moment.

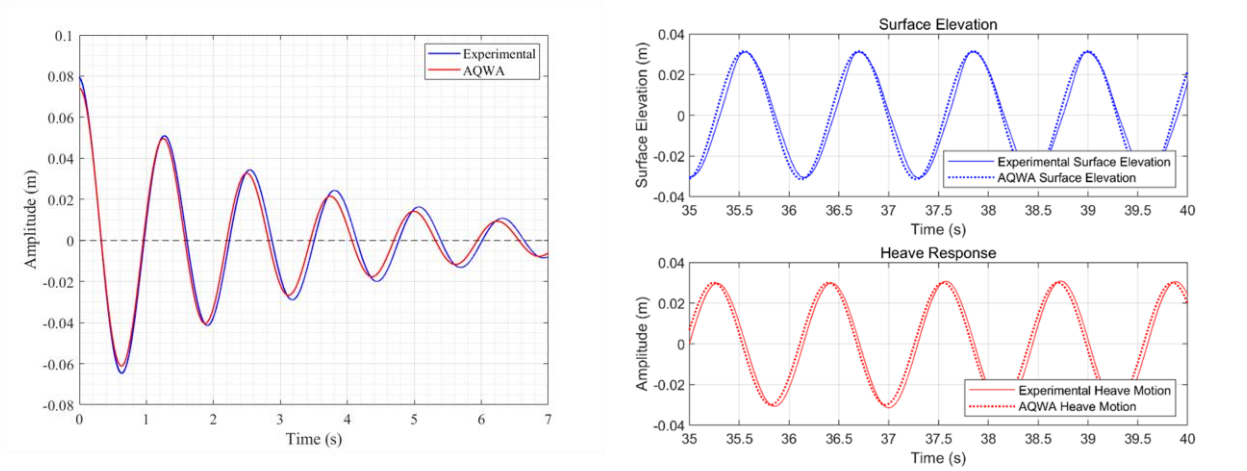

Fig. 5. Heaving WEC validation results. Left: Heave decay test, Right: Heave response in regular incident waves.

B. Numerical Model

To investigate the influence of a WEC's heave and surge motions on OWT wave loading, a theoretical full-scale numerical model was developed. The considered development site was based on the sea state conditions at the *Star of the South* offshore wind farm project located off the Gippsland coast in Victoria, Australia. The *Star of the South* is the first proposed offshore wind farm in Australia and has depth characteristics suitable for monopile structures, ranging from approximately 25 m to 40 m. The water depth selected for the numerical testing was set to 35 m as an intermediate value. Metocean data accessed from [20] and [21] have been used to quantify the expected environmental conditions at the selected site. Data retrieved for various return period intervals have been summarised in Table 1.

OWT and WEC geometry

The physical geometry of the WEC and OWT can be found in Fig. 6 and Table 2 and was a key consideration when developing the numerical model to ensure it is reflective of a realistic co-located system. It is expected that monopile foundations could grow to 10-12 m in diameter and be utilised in water depths greater than 40 metres [17]. An example of an offshore wind farm using the proposed extra-large monopiles is the Hornsea 2 project, which has installed over 100, 9.5 m diameter monopiles [18]. The OWT monopile diameter for this numerical model has been set to 8.0 m as a conservative approach.

TABLE 1
METOCEAN PARAMETERS AT THE SELECTED SITE

Return period (years)	1	100	1000
Operational conditions			
Peak wave period [T_p] (s)	7.30	-	-
Significant wave height [H_s] (m)	1.37	-	-
Survivable conditions			
Peak wave period (s)	8.08	9.30	9.89
Significant wave height (m)	5.50	6.90	7.80
Maximum wave height [H_{max}] (m)	10.77	14.29	16.15
Wind speed (m/s)	29.30	45.20	53.80

The WEC's geometry was based on a cylinder and was sized by adjusting geometrical parameters in Equation (1) [22] (i.e., diameter, draft, etc.) such that the heave natural period (T_3) aligned with the peak wave period (T_p) at the site. Hence, the heave natural period of the system will theoretically match the target operational wave period which is beneficial for energy production.

Heave and surge damping factors (B_{33} and B_{11}, respectively) were variables that were investigated and controlled numerically by adjusting the damping matrix in AQWA (based on methods described in [14]). Note that this damping does not represent a PTO system. All other degrees of freedom (e.g. sway, roll, etc) were numerically deactivated.

$$T_3 = 2\pi \cdot \sqrt{\frac{M_s + A_{33}}{\rho g A_{wp} + k_s}} \qquad (1)$$

$$A_{33} = \frac{2\pi\rho}{3} \cdot \frac{D^3}{8} \qquad (2)$$

Here, M_s is the total mass of the structure; A_{33} is the

TABLE 2
PRINCIPAL PARTICULARS FOR THE TESTED WEC AND OWT

Item	Description	Value
Site	OWT WEC spacing (m)	24.0
	Water depth (m)	35.0
	Wave period range (s)	3.0 – 10.0
	Significant wave height (m)	1.5
OWT	Diameter (m)	8.0
	Submerged length (m)	35.0
WEC	Diameter (m)	18.0
	Draft (m)	10.0
	Free board (m)	4.0
	VCG (from keel) (m)	5.0
	Mass (t)	2500.5
	Mass moments of inertia (I_{xx}, I_{yy}, I_{zz}) (t m^2)	150049, 1371, 150049
Mooring	Unstretched length (m)	25.0
	Axial stiffness (kN m^{-1})	10.0

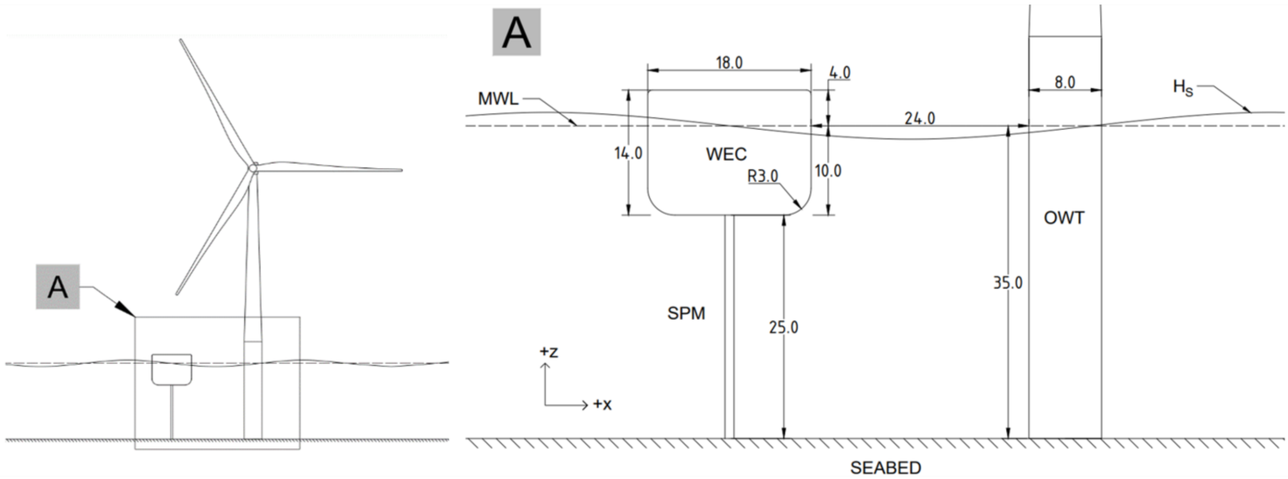

Fig. 6. The geometry of the WEC and OWT used in this numerical investigation.

added mass of the system in heave; ρ is the density of water; g is the acceleration due to gravity; A_{wp} is the waterplane area of the WEC; k_s is the stiffness of the mooring; and D is the diameter of the WEC.

Numerical settings

Numerical parameters for the full-scale model were informed by settings obtained during validation. An additional mesh convergence study was performed to balance computational requirements and the accuracy of results. The convergence study investigated the effect of body mesh size on the maximum pitch moments and surge forces acting on the OWT foundation. The accuracy of each simulation in the convergence study was compared to results obtained from a simulation that used the maximum number of allowable elements as permitted with the available ANSYS licence. For this model, the results converged at a body mesh size of 1.0 m, which produced a relative error of less than 1%. This sizing was found to maintain accuracy while reducing simulation times over finer meshes. The water plane of the numerical model was set to 1000 m × 1000 m. The WEC's station-keeping system was modelled as a single-point mooring (SPM) with a linear spring and is similar in configuration to other point absorber WECs. Pitch moments were measured about the base of the wind turbine, which was located at the sea floor.

Natural periods

Numerical free body decay tests for the WEC's heave and surge motions were performed to verify the respective natural periods. The heave natural period was found to be 7.34 s, which aligns closely with the peak wave period in operational conditions at the site. The surge natural period was 125 s and lies outside typical ocean wave periods as recommended for many offshore structures [22].

Tested conditions

Five conditions were tested to analyse the effect of the WEC's motions on the OWT foundation. The WEC's motions were controlled in the numerical model. The conditions are as follows:

1. OWT (no WEC): Baseline data for comparison.
2. OWT and fixed WEC (no WEC motions).
3. OWT and heaving WEC (1-DOF).
4. OWT and surging WEC (1-DOF).
5. OWT and heave/surge coupled WEC (2-DOF).

Regular waves with periods (T) ranging from 3 to 10 seconds and a wave height (H) of 1.5 metres were simulated to reflect typical operational conditions at the selected site. Damping was applied through the AQWA damping matrix in increasing levels for each condition.

Irregular waves with significant wave heights (H_s) and peak wave periods that align with the metocean dataset for one-year average conditions, one-year maximum conditions and a 100-year maximum condition were also simulated (refer to Table 1). The time series for the irregular sea states were based on the theoretical JONSWAP spectrum and were generated with the methods described in [23]. The time series were then imported into the AQWA software as a user-defined wave.

III. Results and Discussion

The effect of WEC heave motions and damping on OWT wave loading

Results for the heave-only condition are presented in Fig. 7 and show the WEC's heave damping and heave motions (Fig. 8) have a substantial impact on the wave loading imparted to the OWT foundation. As a baseline, the surge forces on the OWT (without WEC) peak at approximately 7 s with a magnitude of 783.3 kN. Whereas the OWT pitch moments (without WEC) show a peak of 21.1 MN·m at approximately 6 s, then display a prominent reduction in moment as the wave periods increase. Increasing levels of heave damping were tested (Fig. 7 and Fig. 8 - represented in greyscale with increasing saturation) and demonstrate the effect heave damping has on OWT wave loading.

When the WEC is introduced, there is a common trend for all conditions (fixed and heaving) on the measured

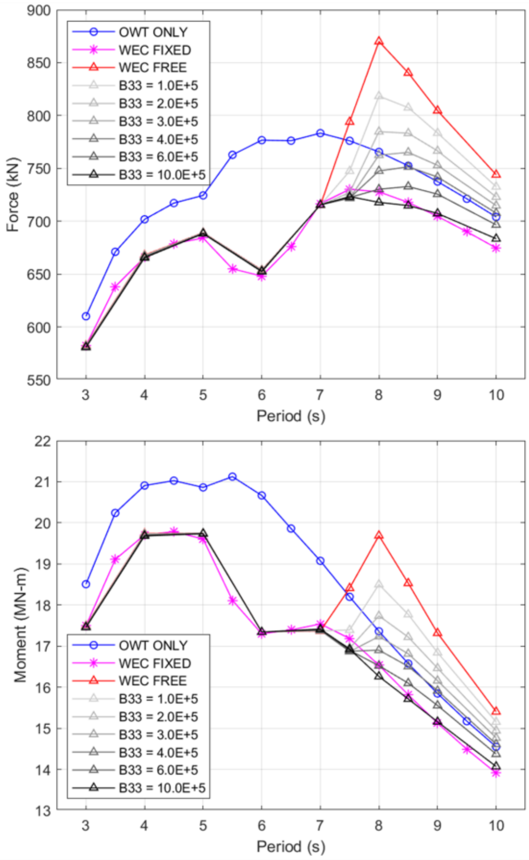

Fig. 7. OWT wave loading with a co-located heaving WEC (1-DOF) showing the effect various damping factors. Top: OWT surge force, Bottom: OWT pitch moment.

OWT surge force and pitch moment. A clear reduction in wave loading for all conditions below 7 s can be observed, however, in wave periods greater than 7 s, the effect of heave damping becomes substantial. The greatest reduction in OWT wave loading occurred when the WEC was fixed or heavily damped. However, as the heave damping is reduced, OWT wave loading begins to increase and eventually surpasses OWT wave loading when the WEC was not installed.

Fig. 8 shows that reducing the heave damping on the WEC had the effect of increasing the WEC's heave motions, particularly as the waves approached the WEC's heave natural period. The OWT also displayed an increasing surge force and pitch moment for these periods. The peak in OWT surge force and pitch moment align with the largest maximum heave displacement. This may be due to radiated waves imparting additional energy onto the OWT foundation.

The effect of WEC surge motions and damping on OWT wave loading

Results for the surge-only condition are presented in Fig. 9 and show the WEC's surge damping and motions create a double peak in the OWT surge force and pitch moment. Regarding OWT surge force, a local maximum for all damped conditions is observed at 4 s and a global

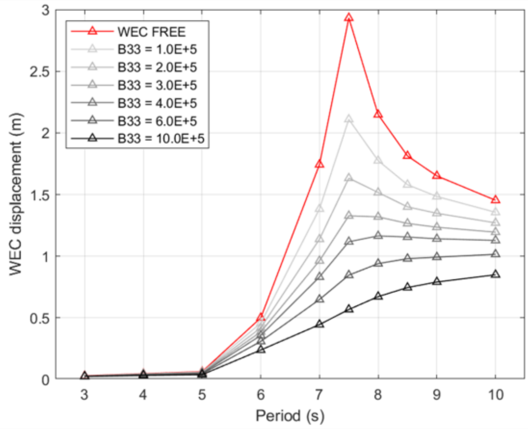

Fig. 8. WEC heave displacement with various levels of heave damping.

maximum is observed at 7.5 s. The pattern is repeated for the OWT pitch moments; however, the local maximum occurs at 7 s and the global maximum occurs at 4 s. A substantial reduction in OWT surge force and pitch moment can be seen between these peaks, where the largest reduction in surge force occurs at 5.5 s and the largest reduction in pitch moment occurs at 6 s. Surge damping has an inverse effect on OWT wave loading across the tested wave periods, where higher levels of damping tend to reduce OWT wave loading in wave periods greater than 6 s, however, lower levels of damping tend to decrease wave loading in wave periods lower than 6 s. It is unclear why this occurs and requires further research.

The effect of coupled WEC motion on OWT wave loading in regular waves

The effects of the WECs coupled heave and surge motions on OWT wave loading is presented in Fig. 10. The coupled simulation combines a moderate level of heave and surge damping (where B_{11} = 4,500,000 N/m/s and B_{33} = 600,000 N/m/s). These damping values were selected as an intermediate between a fully constrained and free-floating WEC. The forces and moments acting on the OWT tend to follow the shape of the surge only damping tests, suggesting the WECs surge motions may have greater influence than the WECs heave motions, however this requires further research to confirm. Overall, coupling heave and surge appears to have a greater effect on OWT wave loads then individual degrees of freedom, and reduces OWT wave loading across a wide range of periods. Nevertheless, both OWT surge force and pitch moments display a peak at 4 s which may potentially relate to wave interactions between the OWT and WEC, again requiring further investigation.

The effect of coupled WEC motion on OWT wave loading in irregular waves

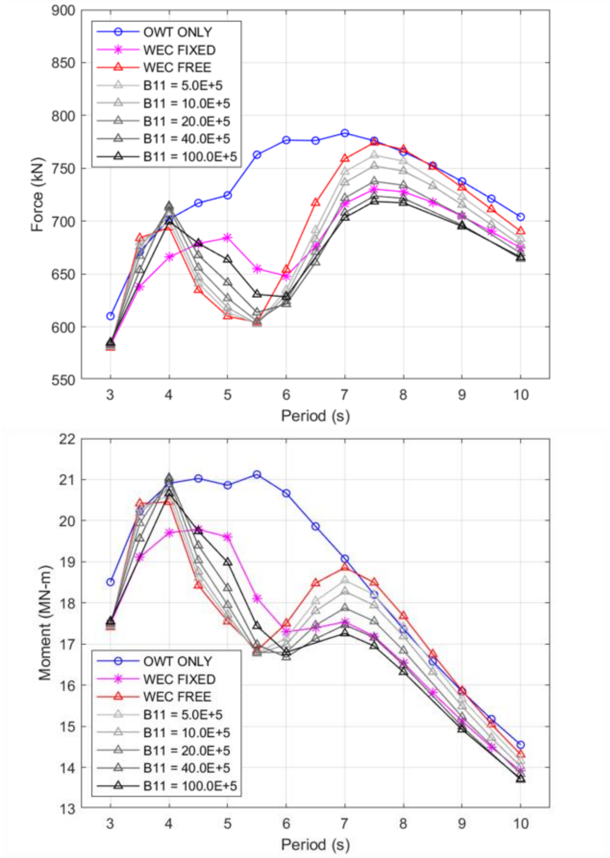

Fig. 9. OWT wave loading with a co-located surging WEC showing the effect various damping factors. Top: OWT surge force, Bottom: OWT pitch moment.

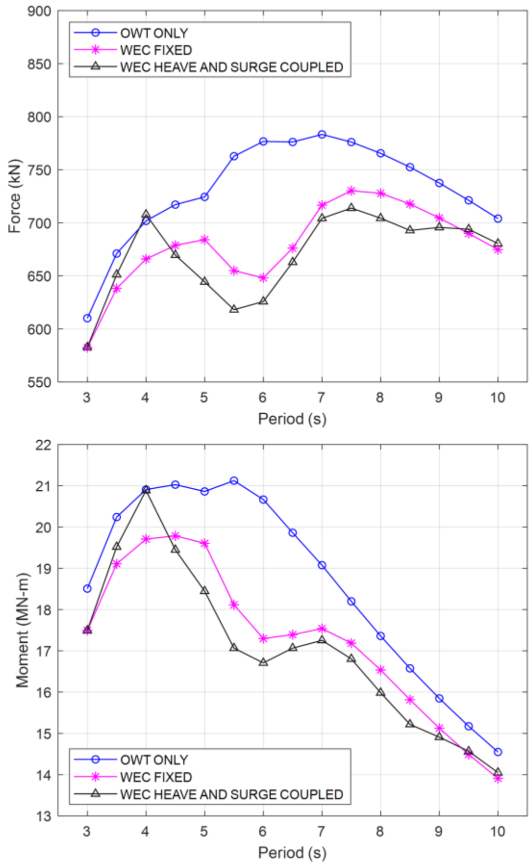

Fig. 10. OWT wave loading with a co-located heave and surge coupled WEC, moderate damping factors were used here. Top: OWT surge force, Bottom: OWT pitch moment.

The effect of heave and surge coupled WEC motions on OWT wave loading in irregular waves is presented in Fig. 11. Damping factors from the previous coupled motion tests were applied for the irregular wave investigation. The sea states were simulated for a three-hour duration. The tested sea states were based on metocean conditions at the site and included a one-year operational condition and a 100-year survivable condition, respectively (Refer to Table 1).

The time-domain response was analysed using spectral analysis, with particular focus on the peak power spectral density (*PSD*). Spectral data from the OWT and WEC conditions were normalised against the OWT-only condition.

Regarding the operational condition (where H_s = 1.5 m and T_p = 7.3 s; Fig. 11 - Top), the fixed WEC was able to reduce peak OWT surge force *PSD* by 10.5%. By contrast, the damped heave and surge coupled WEC was able to reduce peak OWT surge force *PSD* by 33.2%.

Regarding the 100-year return sea state (where H_s = 6.9 m and T_p = 9.3 s; Fig. 11 - Bottom), the fixed WEC was able to reduce peak OWT surge force *PSD* by 9.9%. By contrast, the damped heave and surge coupled WEC was able to reduce peak OWT surge force *PSD* by 19.2%. Clearly, heave and surge coupled WEC motions have a substantial effect on reducing OWT wave loading, however, the effectiveness appears to reduce considerably in survivable conditions. Further research investigating survivable conditions is recommended.

IV. Limitations of the Study

This study did not investigate the effect of the WEC heave or surge phases on OWT wave loading. Findings from [12] indicate that the WEC's phases are critical in reducing wave loading. As such, it is recommended to investigate the effect of the WEC's phases when heave and surge motions are coupled.

V. Conclusions

This paper presents the results of a full-scale numerical study regarding a co-located fixed offshore wind turbine and point absorbing wave energy converter at the proposed *Star of the South* wind farm in Gippsland, Victoria, Australia. This investigation used Ansys AQWA software to investigate how WEC heave and surge motions affect OWT wave loading. The effect of damping on the WEC structural motions was investigated. Both regular and irregular waves were tested with sea state conditions sourced from the installation site. Key findings are as follows:

1. WEC surge motions appear to have a greater influence on reducing OWT wave loading when compared to WEC heave motions.

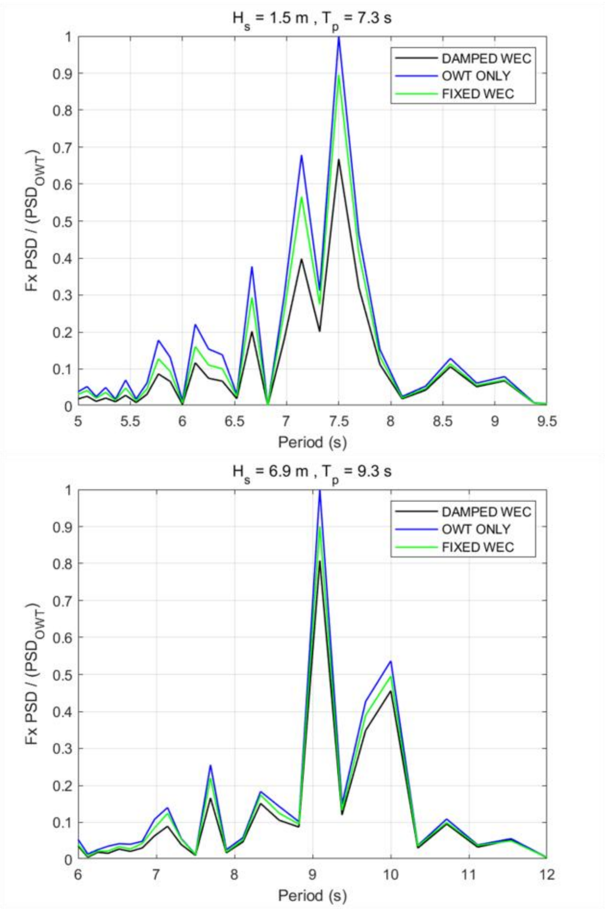

Fig. 11. PSD plots of the OWT wave loading with a heave and surge coupled WEC in irregular waves. Top: operational sea state, Bottom: 100-yr return period sea state.

2. Coupled heave and surge WEC motions appear to have a larger effect on reducing OWT wave loading than heave or surge motions in isolation.

3. Motion damping (not to be confused with PTO damping) plays an important role in reducing OWT wave loading.

4. Regarding irregular sea states, the coupled heave and surge WEC reduced OWT peak PSD wave loading by 33% in operational conditions and 19% for 100-year maximum conditions.

REFERENCES

[1] R. Kukreja, “Various Advantages and Disadvantages of Wave Energy,” Conserve Energy Future, 2023. [Online]. Available: https://www.conserve-energy-future.com/advantages_disadvantages_waveenergy.php [Accessed 22 09 2023]

[2] Perez-Collazo, D. Greaves and G. Iglesias, “A review of combined wave and offshore wind energy,” Renewable and Sustainable Energy Reviews, 42, 141-153, 2014. http://dx.doi.org/10.1016/j.rser.2014.09.032

[3] G. Rinaldi, “Offshore Renewable Energy,” intechopen.com, 9 September 2020. [Online]. Available: https://www.intechopen.com/chapters/71361. https://doi.org/10.5772/intechopen.91662

[4] M. Borg, M. Collu and F. Brennan, “Use of a wave energy converter as a motion suppression,” Energy Procedia, 35, 223-233, 2013. https://doi.org/10.1016/j.egypro.2013.07.175

[5] E. Gaughan and B. Fitzgerald, “An assessment of the potential for Co-located offshore wind and wave,” Energy, 200, 117526, 2020. https://doi.org/10.1016/j.energy.2020.117526

[6] C. Zhao, P. Thies and J. Lars, “System integration and coupled effects of an OWT/WEC device,” Ocean Engineering, 220, 108405, 2020. https://doi.org/10.1016/j.oceaneng.2020.108405

[7] Z. Zeng Hu, T. Mai, D. Greaves and A. Raby, “Investigations of offshore breaking wave impacts on a large offshore structure,” Journal of Fluids and Structures, 75, 99-116, 2017. https://doi.org/10.1016/j.jfluidstructs.2017.08.005

[8] F. Meng, N. Sergiienko, B. Ding, B. Zhou, L. Da Silva, B. Cazzolato and Y. Li, “Co-located offshore wind–wave energy systems: Can motion suppression and reliable power generation be achieved simultaneously?,” Applied Energy, 331, 120373, 2022. https://doi.org/10.1016/j.apenergy.2022.120373

[9] S. Astariz, C. Perez-Collazo, J. Abanades and G. Iglesias, “Hybrid wave and offshore wind farms: A comparative case study of co-located layouts,” International Journal of Marine Energy, 15, 2-16, 2016. https://doi.org/10.1016/j.ijome.2016.04.016

[10] S. Astariz and G. Iglesias, “Co-located wind and wave energy farms: Uniformly distributed arrays,” Energy, 113, 497-508, 15 2016. https://doi.org/10.1016/j.energy.2016.07.069

[11] E. Gubesch, J.-R. Nader, B. Ding, B. Cazzolato, Y. Li, N. Sergiienko and I. Penesis, “Experimental Hydrodynamic Investigation of a Co-located Wind Turbine and Wave Energy Converter,” in International Conference on Ocean, Offshore and Arctic Engineering, Melbourne, 2023.

[12] E. Gubesch, J.-R. Nader, B. Ding, B. Cazzolato, Y. Li, N. Sergiienko and I. Penesis, “Experimental investigation of a co-located wind and wave energy system in regular waves,” Renewable Energy, 219, 119520, 2023, https://doi.org/10.1016/j.renene.2023.119520.

[13] D. Evans, “The Hydrodynamic Performance of a Heaving Only Buoy: An Experimental Study,” NCMEH Final Year Thesis Project, 2019.

[14] A. Pols, E. Gubesch, N. Abdussamie, I. Penesis and C. Chin, “Mooring Analysis of a Floating OWC Wave Energy Converter,” Marine Science and Engineering, 9, 228, 2021. https://doi.org/10.3390/jmse9020228

[15] O. Kennedy, “An Alternative Mooring Tension Prediction Method Using a Neural Network,” NCMEH Final Year Thesis Project, 2022.

[16] Majidiyan, E. Hossein, D. Howe, and E. Gubesch. Part A: Innovative Data Augmentation Approach to Enhance Machine Learning Efficiency—Case Study for Hydrodynamic Purposes. Appl. Sci. 2025, 15(1), 158; https://doi.org/10.3390/app15010158

[17] Boslan Engineering and Consulting, “The next generation monopile foundations for offshore wind turbines,” 01 January 2023. [Online]. Available: https://www.boslan.com/offshore-wind-farms/monopile-foundations

[18] A. Bajic, “Hornsea Two monopile foundations in place,” 10 October 2021. [Online]. Available: https://www.projectcargojournal.com

[19] D. Foxwell, “Seabed surveys underway for Australia’s Star of the South windfarm,” 06 March 2020. [Online]. Available: https://www.rivieramm.com

[20] CSIRO, “National Map,” 2014. [Online]. Available: https://nationalmap.gov.au/about

[21] “MetOceanView Operations and Planning System,” MetOceanView, [Online]. Available: https://www.metoceanview.com/

[22] DNV, “DNV-RP-C205 Environmental conditions and environmental loads - Recommended Practice,” 09 2021. [Online]. Available: https://www.dnv.com/oilgas/download/dnv-rp-c205-environmental-conditions-and-environmental-loads.html

[23] E. Gubesch, N. Abdussamie, I. Penesis and C. Chin, “Physical and numerical modelling of extreme wave conditions,” Ocean Engineering, 283, 115055, 2023. https://doi.org/10.1016/j.oceaneng.2023.115055